The dissociative adsorption of H$_2$ on Cu(100): orientation dependence and impurity effects

The dissociative adsorption of H_2 on Cu(100): orientation dependence and impurity effects

Xie Jianjun†‡§, Jiang Ping†‡§ and Zhang Kaiming†‡§

† CCAST (World Laboratory), PO Box 8730, Beijing 100080, People's Republic of China
‡ Fudan-T D Lee Physics Laboratory, Fudan University, Shanghai 200433, People's Republic of China
§ State Key Laboratory of Applied Surface Physics, Fudan University, Shanghai 200433, People's Republic of China

Abstract. The dissociative adsorption of H_2 on Cu(100) is studied by using the embedded-atom method (EAM). The molecular orientation dependence and the impurity effects have been investigated. It is found that the most favourable molecular orientation for H_2 dissociation is to keep the H–H axis parallel to the surface. In this case, the corresponding activation barrier is lowest. Calculations show that when an impurity atom is present in the Cu substrate, the chemisorption properties near the impurity atom are affected. Ni and Pd can promote the H_2 dissociation by lowering the activation barrier height; Ag, however, impedes the H_2 dissociation since the activation barrier is lifted. Various H_2 dissociation pathways are discussed and the corresponding potential-energy surfaces (PESs) are presented.

1. Introduction

The dissociative adsorption of hydrogen molecules on copper surfaces has received considerable attention both experimentally and theoretically [1–11]. It has been found that hydrogen dissociation on the Cu surface is a typical activated process. The key parameter characterizing this dynamical process is the barrier height of activation. Experimental measurement [1, 2, 12] are made by using the molecular-beam technique to obtain the activation barrier height. Theoretically, one needs to calculate the adiabatic potential-energy surface (PES) to deal with this subject [5, 6, 8–12]. To our knowledge, most of the previous theoretical investigations [5, 6, 9–11] assumed that H_2 dissociates on a substrate of pure metal without any impurities and defects and the H–H axis is always kept parallel to the surface. However, it is practically impossible to remove all the impurities or defects in a real crystal sample. Furthermore, in many industrially important catalytic reactions, some foreign atoms must be intentionally deposited on a given substrate to form a composite catalyst [13, 14] for special use. Besides, the molecular axis orientation in real adsorption processes is not always parallel to the surface. Obviously all these effects on the chemisorption properties should be considered in a more reasonable calculation. Recently, the present authors have successfully extended the embedded-atom method (EAM) [15–17] to treat the interaction between hydrogen molecule and a contaminated Ni surface [18]. The defect effect on the hydrogen dissociation process has been investigated. The results show that the EAM can be conveniently applied to treat molecules near the metal surfaces. Encouraged by this success, in the present paper, we give the calculations for H_2 dissociation on the Cu(100)

surface. Various dissociation pathways, different molecular orientations and impurity effects are considered.

The paper is organized as follows. First the EAM and its extension to the molecule–surface system is briefly outlined in section 2. Then in section 3, the results for H_2 adsorption on the Cu(100) surface are presented with discussion of the effects of molecular orientation and impurity, and finally, in section 4, the main conclusions are summarized.

2. The theoretical model and computational details

The basic equations of EAM are

$$E_{tot} = \sum_i F_i(\rho_{h,i}) + \frac{1}{2} \sum_j \sum_{i,i \neq j} \phi_{ij}(R_{ij}) \tag{1}$$

$$\rho_{h,i} = \sum_{j,(j \neq i)} \rho_j(R_{ij}) \tag{2}$$

where E_{tot} is the total energy and $\rho_{h,i}$ is the electron density at atom i due to all other atoms. ρ_j is the electron density of atom j at the site of atom i, R_{ij} is the distance between atoms i and j, $F_i(\rho_{h,i})$ is the energy to embed atom i in an electron density $\rho_{h,i}$, and ϕ_{ij} is a two-body central potential between atoms i and j.

When we apply the EAM to the present work, a theoretical model is chosen as one hydrogen molecule outside a finite slab of Cu atoms, which consists of six atomic (100) planes, each plane includes 121 Cu atoms. In the slab an impurity atom, which is Ni, Pd or Ag, is assumed to exist substitutionally. The function $F_M(\rho)$ and the pair potential $\phi_{M-M}(R)$ used are quoted from Mei *et al* [17], here the subscript M represents metal atoms. According to [15], the electron density for each metal atom is given as a sum of s and d contributions

$$\rho(r) = N_s \rho_s(r) + (N - N_s)\rho_d(r). \tag{3}$$

where N is the total number of outer electrons, N_s is a parameter which corresponds to the s-like content of the atomic electron density and ρ_s and ρ_d are taken from the calculations of Clementi and Roetti [19].

In order to apply the EAM to H_2–metal interaction, the two-body potentials of ϕ_{H-M} and ϕ_{H-H} must be determined. Within the framework of the EAM, the total energy of H_2 is given by $E_{H_2}^{tot} = 2[F_H(\rho) + \frac{1}{2}\phi_{H-H}(r)]$. Since the exact value of $E_{H_2}^{tot}$ can be obtained experimentally, $\phi_{H-H}(r)$ can be written as

$$\phi_{H-H}(r) = E_{H_2}^{tot}(r) - 2F_H(\rho) \tag{4}$$

where the function $F(\rho)$ is taken of the form [15]

$$F_H(\rho) = b_1\rho + b_2 + 1/(b_3\rho + b_4). \tag{5}$$

The potential $\phi_{H-M}(r)$ is assumed to be

$$\phi_{H-M}(r) = \frac{a_0(1 + a_1 r^{a_2})e^{-a_3 r}}{r}. \tag{6}$$

Table 1. Parameters used in the calculation ($b_1 = 13.5$, $b_2 = -4.0986$, $b_3 = 34.9288$, $b_4 = 0.244$).

	Cu	Ni	Pd	Ag
a_0	10.832	9.80	12.85	12.80
a_1	4.85	21.85	20.95	2.5329
a_2	1.486	2.18	2.10	2.0
a_3	3.09	3.94	3.86	2.7889
N	11	10	10	11
N_s	1.0 [21]	0.85 [15]	0.65 [15]	1.0 [21]

The parameters in equations (5) and (6) are determined by fitting the experimental adsorption heat and bond length of H atoms on metal surfaces. It is found that the two-body potential $\phi_{H-M}(r)$ of equation (6) combined with the function $F_H(\rho)$ gives a good description of the H atom on Ni, Pd, Cu and Ag surfaces [20]. With the above considerations, the EAM can be directly applied to the system of H_2 outside a metal surface. Taking the interaction energy of a free H_2 molecule with the Cu(100) surface infinitely far away ($E_{H_2}^{tot} + E_{Cu}^{tot}$) as zero, the potential energy of H_2 on the Cu surface is obtained as $E_{H_2/Cu}^{tot} - (E_{H_2}^{tot} + E_{Cu}^{tot})$. The cut-off distance in our calculation is taken as 4.0 Å. The values of parameters used in the calculation are given in table 1.

3. Results and discussion

3.1. Molecular dependence

Figure 1 shows the various pathways and different molecular orientations for H_2 dissociation on the Cu(100) surface which have been considered in the present work. The angle θ between the H–H axis and the surface normal is defined in figure 1(b). Figure 2 is the calculated potential-energy surface (PES) for H_2 dissociation via the pathway shown in figure 1(a). In this configuration, the H–H axis is kept parallel to the surface ($\theta = 90°$) during the adsorption process. It can be clearly seen that there is an entrance channel for H_2 adsorption on the Cu surface. When H_2 is infinitely far away from the surface, the H–H distance is 0.74 Å and the potential energy for H_2/Cu(100) is zero (no interaction between them). As H_2 approaches the surface, the H–H bond is progressively weakened while the H–metal bonds are formed. This is an activated process and the calculated barrier height is 0.62 eV. The calculated H–Cu bond is 1.88 Å and the adsorption heat is 0.42 eV (9.66 kcal mol^{-1}). These results are in good agreement with the experimental measurements [1, 22].

Figure 3 is the potential-energy surface (PES) for H_2 adsorption on Cu(100) via the pathway shown in figure 1(c). In this case, the activation barrier is 0.58 eV, slightly lower than that of figure 2. The adsorption heat is 0.43 eV and the H–Cu bond length is 2.08 Å. Comparing with figure 2, figure 3 has a lower activation barrier and a higher adsorption heat, therefore, H_2 might dissociate a little more easily via this pathway than that of figure 1(a).

As mentioned above, in real adsorption cases, the direction of the H–H molecular axis could not be always in the surface-parallel orientation but might deviate from it in varying degrees. Figure 4 gives the PES for the configuration which is same as that shown in figure 2 except the angle $\theta = 70°$. It can be seen that the activation barrier is lifted from 0.62 eV to 0.70 eV. The adsorption heat decreases to -0.08 eV. A higher activation barrier and a negative adsorption heat mean that the corresponding adsorption process occurs with
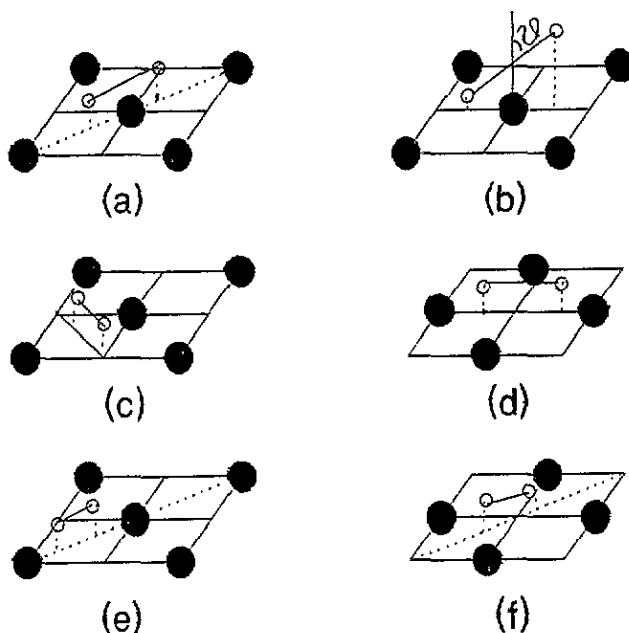
Figure 1. Various dissociation pathways for H_2 on the Cu(100) surface. The solid circles represent Cu atoms; the small empty circles are H atoms. The two H atoms extend (a) from top site to bridge sites, (b) from top site to centre sites, (c) from bridge site to centre sites, (d) from centre site to top sites, (e) from bridge site to top sites, (f) from centre site to bridge sites. The angle θ between the H–H axis and the surface normal is shown in (b).

difficulty. This result can be easily understood by noting the fact that while the H_2 molecules dissociate in a practical process of dissociative adsorption, H–metal bonds must be formed simultaneously. The bond energy of H–Cu is 2.57 eV [23] which is approximately half the H_2 dissociation energy (4.72 eV). Therefore, two H–Cu bonds are needed to form in order to compete with the H–H interaction. However, when the H–H axis deviates from the surface-parallel orientation (particularly in the case of $\theta = 0°$, H–H axis normal to the surface), only one stable H–Cu bond could be formed, which makes dissociation of the H_2 more difficult.

Variations of the activation barrier height (E_a) and the adsorption heat (E_{ad}) with H_2 dissociation pathways and H–H axis orientations are shown in table 2. It can be seen that all the dissociation paths considered fall roughly into two categories: one has a higher activation barrier and a lower adsorption heat, while the other has a lower activation barrier and a higher adsorption heat. For any pathway the activation barrier is lowest in the case of $\theta = 90°$, i.e. the H–H axis parallel to the surface. This is in accord with the experimental observations [3]. For $\theta = 90°$, the calculated E_a is either 0.58 eV or 0.62 eV for different dissociation pathways, which is also in agreement with other theoretical calculations (0.5–0.7 eV) [5, 10, 11]. As the angle θ decreases from 90° to 65°, the activation barrier increases monotonical for all pathways. The variation of E_a is in the range of 0.58–0.74 eV. The experimental value [1] of E_a for H_2 dissociation on Cu surface published recently is 0.622 eV which agrees well with our results. When $\theta = 65°$, the adsorption heat for all pathways becomes negative, this means that in this case the total energy of the H_2/Cu system is
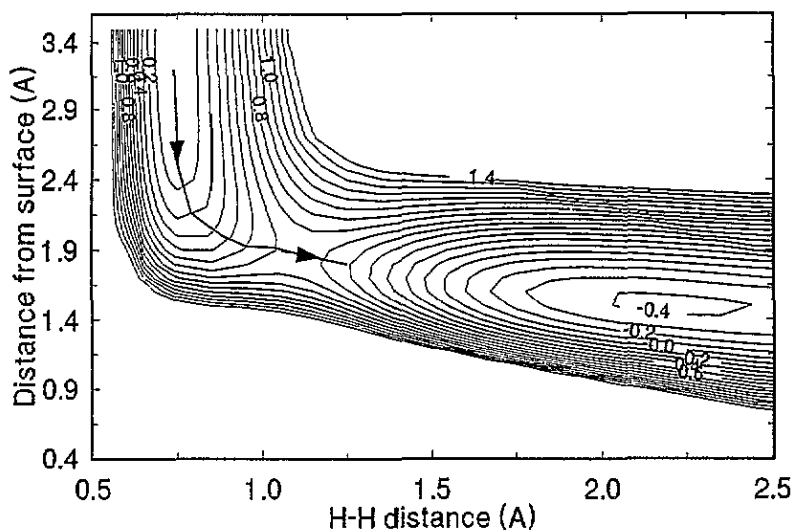
Figure 2. Potential energy contours for H_2 adsorption on Cu(100) via the pathway of figure 1(a). The angle θ between the H–H axis and the surface normal is 90°. The contours are in eV with 0.1 eV intervals.
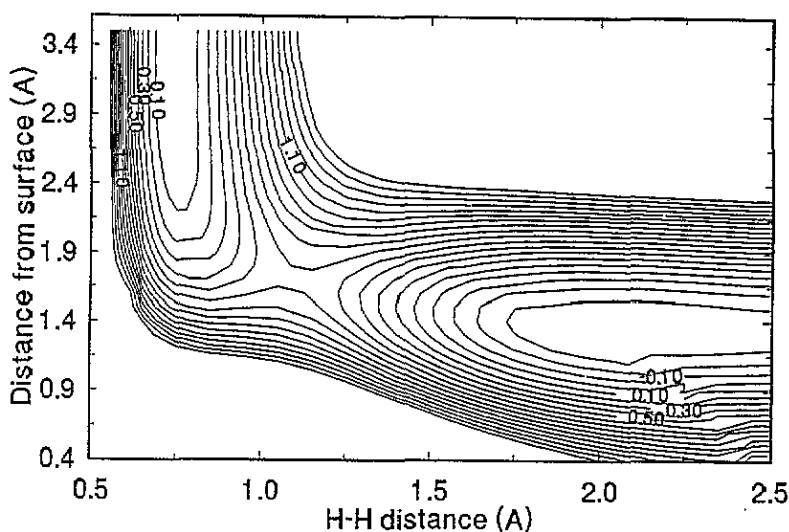

Figure 3. Potential energy contours for H_2 adsorption on Cu(100) via the pathway of figure 1(c), $\theta = 90°$. The contours are in eV with 0.1 eV intervals.

higher than the sum of that of an isolated H_2 and a Cu(100) substrate, therefore the H_2 is difficult to dissociate unless it is excited or perturbed by other exotic energies. It is noted from table 2 that the dissociation pathway from bridge site to the adjacent centre sites gives the highest adsorption heat and almost the lowest activation barrier for any molecular orientations, therefore, we can conclude that this would be the most favourable pathway for H_2 dissociation on the Cu(100) surface.
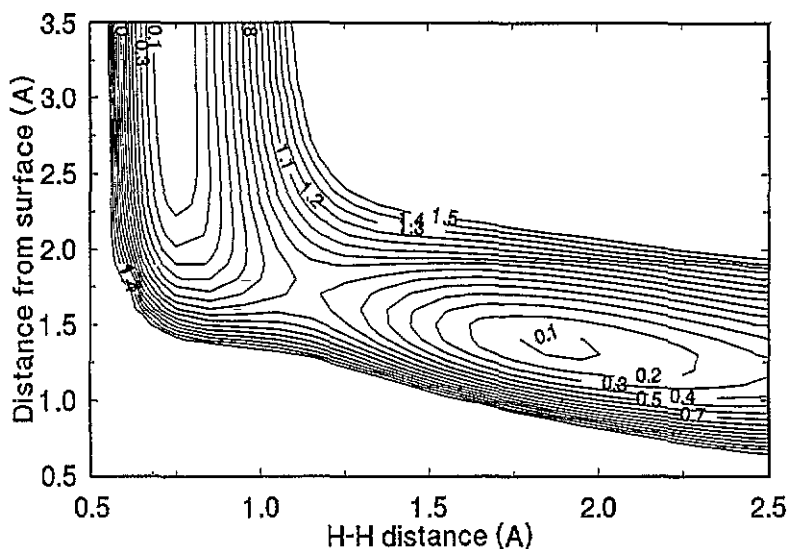
Figure 4. Potential energy contours for H_2 adsorption on Cu(100) via the pathway of figure 1(a), $\theta = 70°$. The contours are in eV with 0.1 eV intervals.

Table 2. Variations of the activation barrier (E_a) and the adsorption heat (E_{ad}) with H_2 dissociation pathways and the molecular orientations. The unit of E_a and E_{ad} is eV.

		θ					
		90°	85°	80°	75°	70°	65°
top site	E_a	0.62	0.63	0.65	0.68	0.71	0.74
to centre sites	E_{ad}	0.42	0.38	0.28	0.13	−0.07	−0.29
top site	E_a	0.62	0.63	0.64	0.66	0.70	0.74
to bridge sites	E_{ad}	0.42	0.38	0.28	0.13	−0.08	−0.29
bridge site	E_a	0.62	0.63	0.65	0.66	0.68	0.72
to top sites	E_{ad}	0.38	0.33	0.19	0.01	−0.19	−0.39
bridge site	E_a	0.58	0.59	0.61	0.62	0.64	0.68
to centre sites	E_{ad}	0.43	0.42	0.36	0.26	0.13	−0.03
centre site	E_a	0.58	0.59	0.60	0.61	0.64	0.67
to bridge sites	E_{ad}	0.42	0.39	0.30	0.18	0.03	−0.12
centre site	E_a	0.58	0.59	0.61	0.62	0.65	0.67
to top sites	E_{ad}	0.40	0.36	0.25	0.11	−0.04	−0.20

3.2. Impurity effects

In this section, we will discuss the effects of impurities on H_2 dissociation on the Cu(100) surface. The possible impurity sites we assumed are shown in figure 5. One dissociation path (from top site to two adjacent bridge sites) as shown in figure 1(a) is chosen to be investigated as a representative. The H–H axis is kept parallel to the surface.

The calculated potential-energy surface for H_2 dissociation on an Ni-contaminated Cu(100) surface is shown in figure 6. One impurity atom Ni is assumed to locate at site 1 of figure 5. In contrast to that shown in figure 2, the activation barrier in figure 6 decreases remarkably from 0.62 eV to 0.22 eV due to the existence of Ni. The adsorption heat is 0.86 eV which is higher than that of pure Cu. This means the impurity Ni promotes
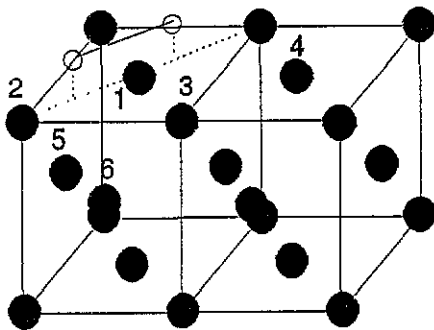
Figure 5. Different impurity sites in the Cu(100) substrate.

the dissociation of adjacent H$_2$. When the impurity atom is Ag instead of Ni, the changes of adsorption property that occur are opposite to the case of Ni, as shown in figure 7. The activation barrier is lifted from 0.62 eV to 0.79 eV, while the adsorption heat is decreased from 0.42 eV to 0.22 eV. Thus, the existence of impurity Ag essentially impedes the dissociation of H$_2$ on the Cu surface.
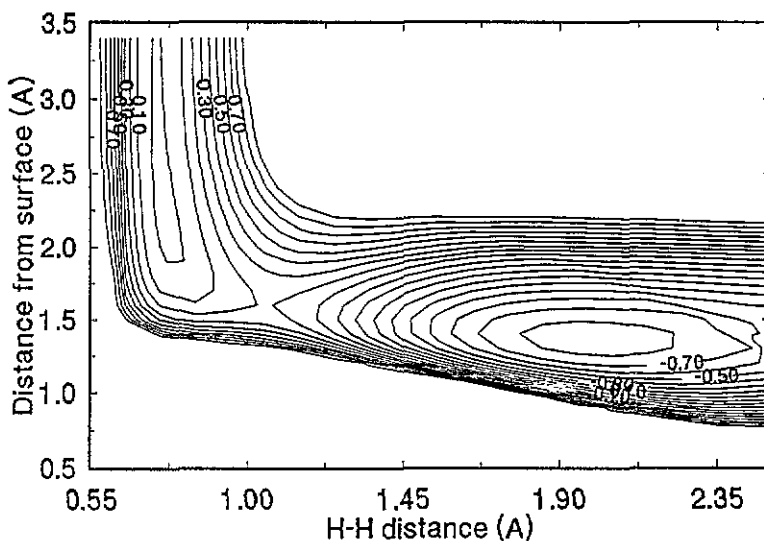

Figure 6. Potential energy contours for H$_2$ dissociation on Ni-contaminated Cu(100) via the pathway of figure 1(a), $\theta = 90°$. The contours are in eV with 0.1 eV intervals.

The calculated activation barriers and the adsorption heats for other impurity sites are listed in table 3 with the results obtained for impurity Pd as well. It is shown that the existence of Pd impurity can also enhance the H$_2$ dissociation by lowering the activation barrier height and lifting the adsorption heat. Comparing with Ni, however, the influence of Pd on H$_2$ dissociation is less significant. From table 3, it can be seen obviously that as the impurity atom moves away from site 1, the effects on H$_2$ dissociation decrease rapidly. When the impurity is located at site 4 or the sub-layer sites 5 and 6, the adsorption of H$_2$
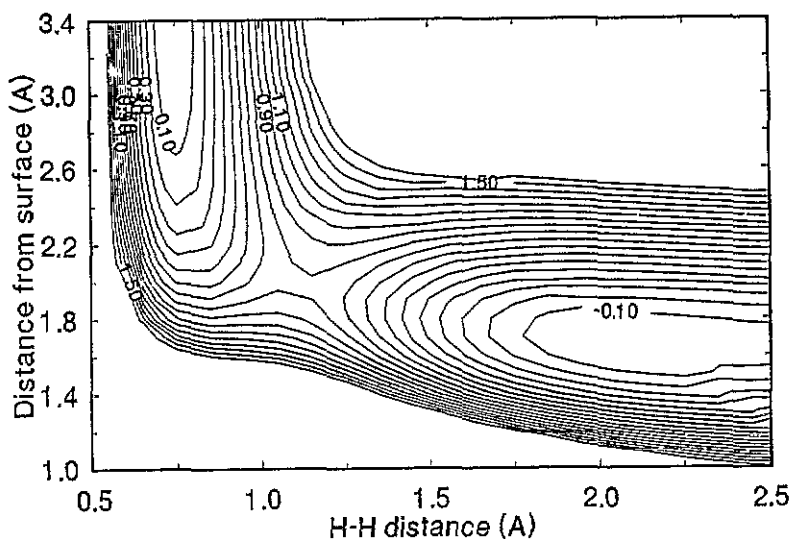
Figure 7. Potential energy contours for H_2 dissociation on Ag-contaminated Cu(100) via the pathway of figure 1(a), $\theta = 90°$. The contours are in eV with 0.1 eV intervals.

Table 3. Activation barriers E_a and adsorption heats E_{ad} for H_2 dissociation on the Cu(100) surface with an impurity atom substitutionally located at different sites. The unit of E_a is eV.

		Impurity site					
		1	2	3	4	5	6
Cu(Ni)	E_a	0.20	0.60	0.61	0.62	0.62	0.62
	E_{ad}	0.86	0.41	0.42	0.42	0.42	0.42
Cu(Pd)	E_a	0.47	0.61	0.61	0.62	0.62	0.62
	E_{ad}	0.55	0.40	0.42	0.42	0.42	0.42
Cu(Ag)	E_a	0.79	0.65	0.64	0.62	0.62	0.62
	E_{ad}	0.22	0.24	0.39	0.42	0.42	0.42

is almost the same as that on a pure Cu surface, i.e. the impurity effect is negligible. This result is similar to the previous findings [18] and the reasons are explained therein.

As to the reasons that different impurities on the Cu surface behave differently, we think the most plausible explanation is their different electronic configurations. According to the values of N and N_s listed in table 1, the effective electronic configurations for Ni, Pd and Cu are $3d^{9.15}4s^{0.85}$, $4d^{9.35}5s^{0.65}$ and $3d^{10}4s^1$ respectively. It is found [5, 6, 18] that the d holes (the unfilled fraction of d bands) are responsible for the decrease of the activation barriers. Here, the number of d holes for Ni, Pd and Cu is 0.85, 0.65 and 0.0 respectively, therefore, the impurity Ni and Pd would give lower activation barriers than Cu. On the other hand, the electronic configuration of Ag is $4d^{10}5s^1$; the d-hole is zero, which is the same as that of Cu. However, their radius density distributions are different as shown in figure 8. It is known [5] that the activation barrier originates from the Pauli repulsion between the closed shell of H_2 and the s electrons of the metal in the process of H_2 approaching the metal surface. It can be seen from figure 8 that the density of s electrons of Ag is higher than that of Cu in the region where s electrons are significant, which results in a stronger Pauli repulsion and a slightly higher activation barrier as H_2 approaches the Ag contaminated Cu surface.
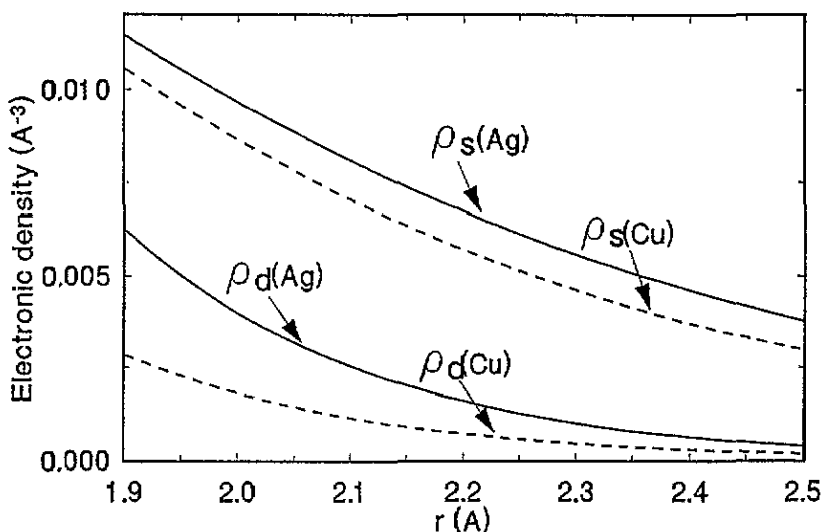
Figure 8. Electron density distributions of Cu and Ag atoms.

4. Conclusions

Following earlier theoretical studies of H_2 dissociative adsorption on Ni(100), we have presented the recent calculations for H_2 on the Cu(100) surface. The molecular orientation dependence and the impurity effects are investigated. It is found that the activation barrier height is lowest in the case where the H–H axis kept parallel to the surface. The existence of the impurity atoms Ni and Pd can promote the dissociation of H_2, while the Ag impurity has the opposite effect. The influence of the impurity on H_2 dissociation decreases rapidly as the impurity atom moves away from the adsorption site.

The agreement of the present results with the experimental measurements and other theoretical calculations indicates that the EAM potential describes fairly well the molecule–surface interactions, and can be easily extended to future investigations of molecule–surface dynamics.

References

[1]   Campbell J M and Campbell C T 1991 *Surf. Sci.* **259** 1
[2]   Anger G, Winkler A and Rendulic K D 1989 *Surf. Sci.* **220** 1

[3]   Rechtien J-H, Harder R, Herrmann G and Snowdon K J 1992 *Surf. Sci.* **272** 240
[4]   Rettner C T, Auerbach D J and Michelsen H A 1992 *Phys. Rev. Lett.* **68** 2547
[5]   Harris A J 1988 *Appl. Phys.* A **47**, 68; 1989 *Surf. Sci.* **221** 335
[6]   Harris J and Andersson S 1985 *Phys. Rev. Lett.* **55** 1583
[7]   Darling G R and Holloway S 1991 *Surf. Sci. Lett.* **244** L81; 1990 *J. Chem. Phys.* **93** 9145
[8]   Michelsen H A and Auerbach D J 1991 *J. Chem. Phys.* **94** 7502
[9]   Norskov J K 1989 *J. Chem. Phys.* **90** 7461
[10] Kutchenhoff S, Brenig W and Chiba Y 1991 *Surf. Sci.* **245** 389
[11] Halsted D and Holloway S 1990 *J. Chem. Phys.* **93** 2859
[12] Balooch M, Cardillo M J, Miller D R and Stickney R E 1994 *Surf. Sci.* **46** 358
[13] Schwab G M 1978 *Adv. Catal.* **27** 1
[14] Kunz A B, Guse M P and Blint R J 1976 *Int. J. Quantum Chem. Symp.* **10** 283
[15] Daw M S and Baskes M I 1984 *Phys. Rev.* B **29** 6443
[16] Foiles S M 1985 *Phys. Rev.* B **32** 7685
      Daw M S 1988 *Phys. Rev.* B**39** 7441
[17] Mei J, Davenport J W and Fernando G W 1990 *Phys. Rev.* B **43** 4653
[18] Xie J J, Jiang P and Zhang K M 1994 *J. Phys.: Condens. Matter* **6** 1219
[19] Clementi E and Roetti C 1974 *At. Data Nucl. Data Tables* **14** Nos 3 and 4
[20] Xie J J, Jiang P and Zhang K M to be published
[21] Harrison W A 1980 *Electronic Structure and the Properties of Solids* (San Fransisco: Freeman) ch 20, p 498
[22] Alexander C S and Pritchard J 1972 *J. Chem. Soc. Faraday Trans.* I **68** 202
[23] The bond energy of H–Cu is $(E_{ad} + E_{diss})/2$: E_{ad} is the adsorption heat and E_{diss} is the dissociation energy of H_2.